

A crack localization method for beams via an efficient static data based indicator

O. Yazdanpanah^a, S. M. Seyedpoor^{a,*}

^aDepartment of Civil Engineering, Shomal University, Amol, Iran

Received 18 October 2013; accepted in revised form 15 February 2014

Abstract

In this paper, a crack localization method for Euler-Bernoulli beams via an efficient static data based indicator is proposed. The crack in beams is simulated here using a triangular variation in the stiffness. Static responses of a beam are obtained by the finite element modeling. In order to reduce the computational cost of damage detection method, the beam deflection is fitted through a polynomial function using a limited number of nodal displacements. A damage indicator based on static responses obtained for healthy and damaged structure is proposed to identify the damage. Three test examples including a simply supported beam, an overhanging beam and an indeterminate beam are considered. The influence of many parameters may affect the efficiency of the method such as the number of elements, the value, type and location of applied load as well as the noise effect is investigated. Numerical results show that, the locations of single and multiple damage cases having different characteristics can be well determined by the method proposed.

Keywords: Crack modeling, damage detection, beam structure, static responses, damage indicator

1. Introduction

Many structural systems may experience some local damage during their lifetime. If the local damage is not identified timely, it may lead to a terrible outcome. Therefore, structural damage detection is of a great importance, because early detection and repair of damage in a structure can increase its life and prevent from an overall failure. Structural damage detection techniques address the problem of how to detect damage that occurred in a structure by using the changes observed in dynamic and static characteristics of the structure. During the last years, much progress has been made to introduce a proper damage detection method for beam structures. For damage detection, the responses of a structure including static and dynamic responses perform a vital role. Several studies related to using dynamic responses such as the

*Corresponding author. Tel and Fax: +98 121 2203726
E-mail address: s.m.seyedpoor@gmail.com

natural frequencies and mode shapes of a structure can be found in the literature [1-13]. Also, damage detection methods based on employing static data have attracted much attention. Since static methods only depend on the stiffness matrix, therefore relations are easier with less complexity. In addition, static techniques have more accurate data, inexpensive tools of measurement and also the speed of access to the right data in comparison with dynamic ones. Banan *et al.* [14] proposed an algorithm for estimating member constitutive properties of the finite element model from measured displacements under a known static loading. The algorithm was based on the concept of minimizing an index of discrepancy between the model and measurements using the constrained least-square minimization. A method for estimating parameters in the linearly elastic structures using the measurements of strain energy was introduced by Sanayei and Saletnik [15]. A structural damage identification algorithm using static test data and changes in natural frequencies has been presented by Wang *et al.* [16]. They used an efficient and simple damage identification technique having two main stages, which employed the structural static deformation and the first a few natural frequencies. The results revealed the efficiency of the proposed algorithm for the damage identification. Bakhtiari-Nejad *et al.* [17] presented a method using static test data. They used a method based on stored strain energy in elements in order to select the loading location. Also, they tested the method experimentally using a frame in order to determine damage at element level without having an accurate model for healthy structure. A two-stage damage detection method based on a grey system theory for damage localization and an optimization technique for damage quantification using the measured static displacement of a cantilever beam was proposed by Chen *et al.* [18]. They showed that the grey relation analysis based method can localize the slight to moderate damage and the optimization can identify the damage magnitude with a high accuracy. Crack detection in elastic beams by static measurement has been made by Caddemi and Morassi [19]. The method can be used to identify single crack in a beam by the knowledge of the damage-induced variations in the static deflection of the beam. They showed that numerical results are in a good agreement with the proposed theory. A parametric study using static response based displacement curvature for damage detection of beam structures has been made by Abdo [20]. The results exhibited that changes in displacement curvature can be used as a good damage indicator even for a small amount of damage. Seyedpoor and Yazdanpanah [21] have been proposed an efficient indicator named SSEBI for structural damage localization using the change of strain energy based on static noisy data". The acquired results clearly showed that the proposed indicator can precisely locate the damaged elements.

The main purpose of this study is to assess the efficiency of a static data based damage detection method for determining the location of damage in beams. For this, an efficient damage indicator is introduced to estimate the damage locations in beam structures. The influence of many parameters affecting the efficiency of the method is investigated. Numerical results demonstrate that the proposed index can well determined the locations of single and multiple damage cases having different characteristics.

2. Damage detection techniques

There are various damage detection techniques that can be utilized to identify the damage in a beam structure. In this section, three more efficient methods including curvature method, flexibility method and strain energy method are described briefly.

2.1. Curvature method

In solid mechanics, the curvature $\frac{1}{\rho}$ (ρ is the radius of curvature) and deflection y can be related as [22,23]:

$$\frac{1}{\rho} = \frac{\frac{d^2 y}{dx^2}}{\left[1 + \left(\frac{dy}{dx}\right)^2\right]^{3/2}} = \frac{M(x)}{EI(x)} \quad (1)$$

where M is the bending moment, E is the modulus of elasticity and I is the moment of inertia of the cross section. Neglecting the second order of slope, the curvature can be approximated by equation (2):

$$\frac{1}{\rho} \approx y'' = \frac{d^2 y}{dx^2} \quad (2)$$

Then, the relationship between curvature, bending moment and stiffness can be considered as follows:

$$\frac{d^2 y}{dx^2} = \frac{M(x)}{EI(x)} \quad (3)$$

Equation (3) shows that the curvature is a function of stiffness. Any change in the stiffness due to any damage at a section may be evidenced by a change in curvature at that location.

2.2. Flexibility method

The flexibility method [3] is a vibration based damage identification method. Using information of a modal analysis, the flexibility change of a structure before and after damage can be considered as an index for identifying structural damage. The modal flexibility matrix of a structure with nd total degree of freedoms can be given by [3]

$$[\mathbf{F}] = [\varphi][1/\omega^2][\varphi]^T = \sum_{j=1}^{nd} \frac{1}{\omega_j^2} \varphi_j \varphi_j^T \quad (4)$$

where $[\mathbf{F}]$ is the modal flexibility matrix; $[\varphi]$ contains the mass normalized mode shape vectors; and $[1/\omega^2]$ is a diagonal matrix containing the reciprocal of the square of circular frequencies in ascending order. Also, ω_j and φ_j are j th circular frequency and mode shape of the structure, respectively. Theoretically, damage reduces the stiffness and then increases the flexibility of the structure. Increase in the structural flexibility can therefore serve as a good indicator for structural damage detection.

2.3. Strain energy method

The strain energy method [9] is another damage identification technique that has been widely used. Assuming that a 2D-beam is divided in n elements, the strain energy stored by an element due to flexural deformation can be expressed as [9]:

$$SE_i = \frac{1}{2} \int_{x_j}^{x_{j+1}} EI(x) \left(\frac{d^2y}{dx^2}\right)^2 dx \tag{5}$$

where x_j and x_{j+1} delimit the element j .

Hypothetically, the damage occurrence leads to increasing the strain energy and therefore can be used as an efficient indicator for damage detection.

3. Crack modeling

As shown in Figure 1, a transverse surface crack is located at x_{cr} from the left end of a beam. A fully open transverse surface crack model, as illuminated by Sinha *et al.* [24], is adopted in this paper. The effect of the crack on the mass is small and can be neglected. The crack only leads to local stiffness reduction in a specified length adjacent to the crack. It is assumed that the reduction of stiffness due to the crack is inside one element. Considering one cracked element as shown in Figure 2, the flexural rigidity EI of the cracked element varies linearly from the cracked position towards both sides in an effective length l_c . The stiffness matrix of the damaged element can be represented as [24]:

$$K_c^e = K_u^e - \Delta K_c^e \tag{6}$$

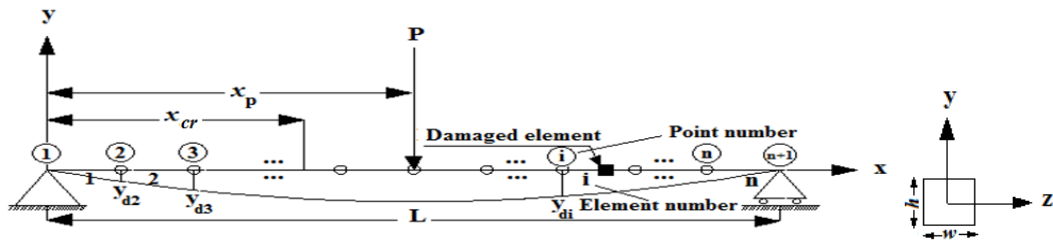


Figure 1. A simply supported beam having a crack located at x_{cr} from the left end

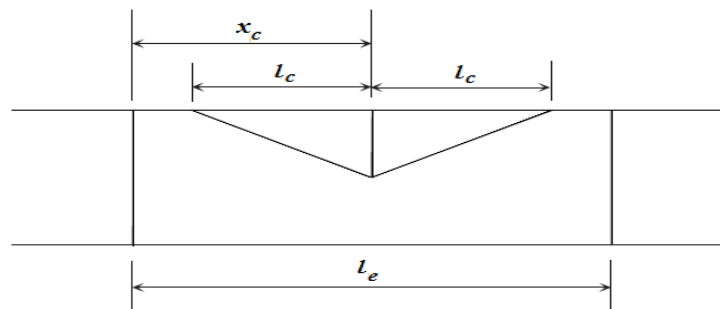


Figure 2. Variation of EI due to the crack in an element with l_e

where K_u^e represents the element stiffness matrix of the intact element; ΔK_c^e is the stiffness reduction on the intact elemental stiffness matrix due to the crack. According to Euler–Bernoulli beam element, the elemental stiffness matrix of the intact beam is expressed as [24]:

$$K_u^e = \frac{2EI_o}{l_e^3} \begin{bmatrix} 6 & 3l_e & -6 & 3l_e \\ & 2l_e^2 & -3l_e & l_e^2 \\ \text{symmetric} & & 6 & -3l_e \\ & & & 2l_e^2 \end{bmatrix} \quad (7)$$

By using the linear variation of EI as proposed by Sinha *et al.* [24], the reduction on the elemental stiffness matrix can be obtained as:

$$\Delta K_c^e = \begin{bmatrix} \Delta K_{11} & \Delta K_{12} & -\Delta K_{11} & \Delta K_{14} \\ & \Delta K_{22} & -\Delta K_{12} & \Delta K_{24} \\ \text{symmetric} & & \Delta K_{11} & -\Delta K_{14} \\ & & & \Delta K_{44} \end{bmatrix} \quad (8)$$

where the stiffness factors are given by

$$\begin{aligned} \Delta K_{11} &= \frac{12E(I_o - I_c)}{l_e^4} \left[\frac{2l_c^3}{l_e^2} + 3l_c \left(\frac{2x_c}{l_e} - 1 \right)^2 \right], \\ \Delta K_{12} &= \frac{12E(I_o - I_c)}{l_e^3} \left[\frac{l_c^3}{l_e^2} + l_c \left(2 - \frac{7x_c}{l_e} + \frac{6x_c^2}{l_e^2} \right) \right], \\ \Delta K_{14} &= \frac{12E(I_o - I_c)}{l_e^3} \left[\frac{l_c^3}{l_e^2} + l_c \left(1 - \frac{5x_c}{l_e} + \frac{6x_c^2}{l_e^2} \right) \right], \\ \Delta K_{22} &= \frac{12E(I_o - I_c)}{l_e^2} \left[\frac{3l_c^3}{l_e^2} + 2l_c \left(\frac{3x_c}{l_e} - 2 \right)^2 \right], \\ \Delta K_{24} &= \frac{12E(I_o - I_c)}{l_e^2} \left[\frac{3l_c^3}{l_e^2} + 2l_c \left(2 - \frac{9x_c}{l_e} + \frac{9x_c^2}{l_e^2} \right) \right], \\ \Delta K_{44} &= \frac{2E(I_o - I_c)}{l_e^2} \left[\frac{3l_c^3}{l_e^2} + 2l_c \left(\frac{3x_c}{l_e} - 1 \right)^2 \right]. \end{aligned} \quad (9)$$

where x_c is the crack location in the local coordinate, l_e is the length of the element and l_c is the effective length of the stiffness reduction. The value of l_c is assumed to be 1.5 times the beam height as illustrated by Sinha *et al.* [24]. Also, E is the Young’s modulus, $I_o = wh^3/12$ and $I_c = w(h - h_c)^3/12$ are the moment of inertia of the intact and cracked cross sections, respectively, w and h are the width and height of the intact beam and h_c is the crack depth. For cases of more than one cracked elements, the same procedure can be followed. The global stiffness matrix K_c is obtained by assembling the element stiffness matrices including those of cracked elements.

4. The proposed damage detection method

In this paper, damage detection of a prismatic beam with a specified length is studied. First, the beam is divided into a number of finite elements. Then, nodal displacements of the beam in measurement points are evaluated using the finite element method. Deformation equation (y) can be obtained by fitting a polynomial curve via specified nodal displacements. By having the deformation equation, the equation of the slope ($\theta = dy/dx$) can be achieved. The displacement curvature equation of healthy beam can now be determined with differentiating the slope equation. This process can also be repeated for damaged beam. It should be noted in this paper, it is assumed that the damage decreases the stiffness and therefore is simulated by a reduction in the moment of inertia (I) at the location of damage. It is also supposed that the damage is occurred in the center of an element. Finally, using the static responses (nodal displacements, slope and displacement curvature) obtained for two above states a new index is introduced that can be utilized to identify the damage.

The step by step summary of the damage detection method can be described as follows:

1) Divide the beam subjected to an arbitrary concentrated load into n elements ($n+1$ nodes) as shown in Figure 3, (x_p is the location of concentrated load from the left side of the beam).

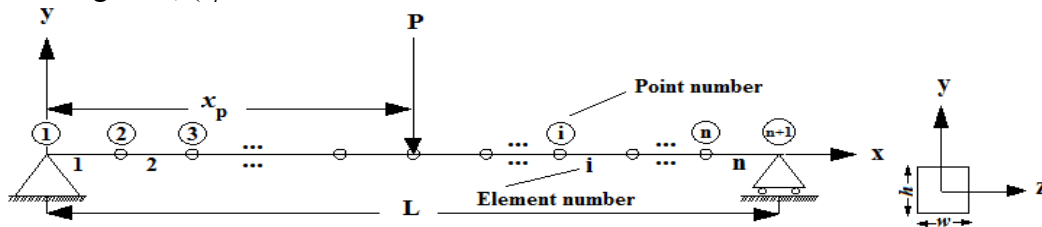


Figure 3. (a) The geometry of simply supported intact beam (b) Cross-section of the beam

2) Analyze the beam using the finite element method for determining the displacements of measurement points shown in Figure 4.

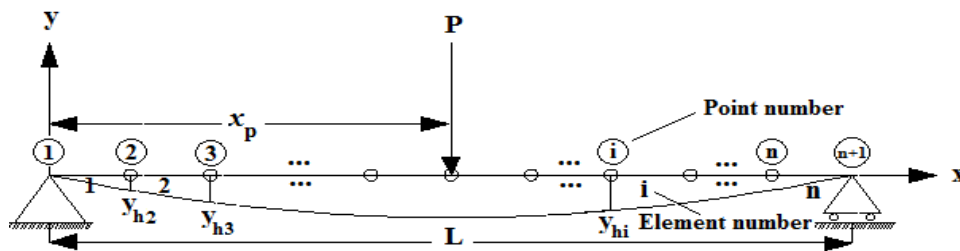


Figure 4. Displacements of the simply supported intact beam under a concentrated load

3) Consider the nodal coordinates and displacements obtained as follows:

$$[x, y_h] = [(x_1, y_{h1}), (x_2, y_{h2}), (x_3, y_{h3}), \dots, (x_i, y_{hi}), \dots, (x_{n+1}, y_{h(n+1)})]$$

Now the goal is to obtain the best curve which passes through the determined points. A polynomial curve that passes through above points can be defined as follows:

$$y_h = \sum_{j=0}^m a_{j+1} x^j = a_1 + a_2 x^1 + a_3 x^2 + a_4 x^3 + \dots + a_{m+1} x^m \tag{10}$$

where $(a_1, a_2, a_3, \dots, a_{m+1})$ are the polynomial coefficients and m is the polynomial degree.

4) Determine the slope (θ) equation with differentiating from equation (10).

$$\theta_h = \frac{dy_h}{dx} = \sum_{j=1}^m (j)(a_{j+1}x^{j-1}) = a_2 + 2a_3x + 3a_4x^2 + \dots + ma_{m+1}x^{m-1} \quad (11)$$

5) Determine the displacement curvature of healthy beam with differentiating from equation (11).

$$\kappa_h = \frac{1}{\rho_h} = y_h'' = \frac{d\theta_h}{dx} = \sum_{j=2}^m (j-1)(j)(a_{j+1}x^{j-2}) = 2a_3 + 6a_4x + \dots + (m-1)ma_{m+1}x^{m-2} \quad (12)$$

The curvature of the beam can now be evaluated at any arbitrary point.

6) Induced a hypothetical damage in an arbitrary element as shown in Figure 1, and analyze the beam for determining the nodal displacements in measurement points.

7) Consider the nodal coordinates and displacements of damaged beam as follows:

$$[x, y_d] = [(x_1, y_{d1}), (x_2, y_{d2}), (x_3, y_{d3}), \dots, (x_i, y_{di}), \dots, (x_{n+1}, y_{d(n+1)})]$$

The displacement curve of damaged beam can be fitted as

$$y_d = \sum_{j=0}^m a_{j+1}x^j = a_1 + a_2x^1 + a_3x^2 + a_4x^3 + \dots + a_{m+1}x^m \quad (13)$$

8) Determine the slope (θ) equation with differentiating from equation (13).

$$\theta_d = \frac{dy_d}{dx} = \sum_{j=1}^m (j)(a_{j+1}x^{j-1}) = a_2 + 2a_3x + 3a_4x^2 + \dots + ma_{m+1}x^{m-1} \quad (14)$$

9) Determine the displacement curvature of damaged beam with differentiating from equation (14).

$$\kappa_d = \frac{1}{\rho_d} = y_d'' = \frac{d\theta_d}{dx} = \sum_{j=2}^m (j-1)(j)(a_{j+1}x^{j-2}) = 2a_3 + 6a_4x + \dots + (m-1)ma_{m+1}x^{m-2} \quad (15)$$

The curvature of the damaged beam can now be evaluated at any arbitrary point.

10) Use the proposed damage index bellow for damage localization.

$$SRBI = \left| \left[(|\kappa_d - \kappa_h|) \times y_d^2 \right] - \left[(|\theta_d| - |\theta_h|)^2 \times y_h \right] \right| \quad (16)$$

In order to improve the *SRBI* (static response based index), the index can be scaled through equation (17) as:

$$nSRBI = \max \left[0, (SRBI - \text{mean}(SRBI)) / \text{std}(SRBI) \right] \quad (17)$$

where mean ($SRBI$) and std ($SRBI$) represent the mean and standard deviation of $SRBI$, respectively. Also, the mean of equation (17) for the mn load conditions can now be selected as an efficient damage indicator as:

$$mnSRBI = \frac{\sum_{c=1}^{mn} nSRBI}{mn} \quad (18)$$

5. Numerical examples

In order to assess the efficiency of the proposed index for damage detection, three test examples including a simply supported beam, an overhanging beam and an indeterminate beam are considered. Various parameters that may affect the performance of the method are studied.

5.1. Example 1: a simply supported beam

A simply supported beam with span $L=1$ (m) shown in Figure 5 is selected as the first example. The beam has a square cross-section with dimensions of 0.2×0.2 m. Modulus of elasticity is $E = 210 GPa$. As shown in Figure 6, for assessment of the method, seventeen different damage scenarios are considered. The first twelfth scenarios (cases 1-12), consist of a single damage under concentrated load. For damage scenarios 1-12, three different load cases as given in Tables 1-3 are considered. The Table 1, Table 2 and Table 3 are used to scenarios 1-8, scenarios 9-10 and scenarios 11-12, respectively.

The thirteenth to fifteenth scenarios (cases 13-15), include multiple damage cases with different intensities. The sixteenth and seventeenth scenarios (case 16 and 17) are considered for single and multiple damages under uniformly distributed load, respectively. The seventh and eighth scenarios (case 7 and 8) are introduced to consider the measurement noise effect.

One of the important parameter for accurately identifying damage is the number of measurement points for static response data. In order to consider this effect, two different finite element meshes are used for the beam in scenarios 1 to 10. The first mesh consists of 10 elements for the beam (damage scenarios 1-8, the length of each element is equal $0.1 L$). The second mesh models the beam with 20 elements (damage scenarios 9-10, the length of each element is equal $0.05 L$). The influence of value of load is also considered here. The eleventh and twelfth cases (scenario 11 and 12) is similar to the second and third cases, but, the load value is two times. In fact, this case is considered for investigating the effect of load value on damage detection. Practically, the measurement noise can not be avoided. Hence, in order to consider the noise effect, the nodal displacements of the damaged structure are randomly polluted by a uniformly distributed number as:

$$dis_n^d = dis^d \times [1 + (2 \text{ rand} - 1) \times \text{noise}] \quad (19)$$

where dis^d stands for the nodal displacements of the damaged structure, dis_n^d represents the noisy nodal displacements and rand is a random number uniformly generating between 0 and 1. Also, noise is the percentage of noise considered. In this example, 3% noise is assumed.

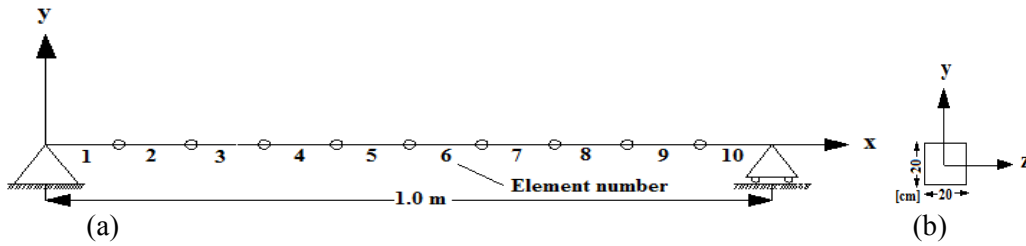


Figure 5. (a)Geometry of the simply supported beam; (b) Cross-section of the beam

Table 1. Static load cases applied to the simply supported beam (scenarios 1-8)

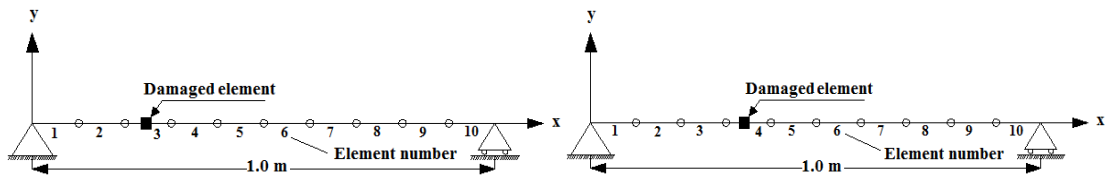
Node	Case 1 (KN)	Case 2 (KN)	Case 3 (KN)
	P_v	P_v	P_v
3	-10	0	0
6	0	-10	0
9	0	0	-10

Table 2. Static load cases applied to the simply supported beam (scenarios 9-10)

Node	Case 1 (KN)	Case 2 (KN)	Case 3 (KN)
	P_v	P_v	P_v
5	-10	0	0
11	0	-10	0
17	0	0	-10

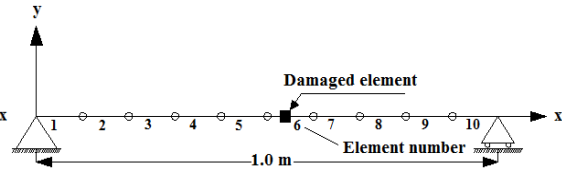
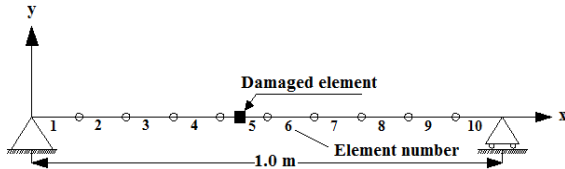
Table 3. Static load cases applied to the simply supported beam (scenarios 11-12)

Node	Case 1 (KN)	Case 2 (KN)	Case 3 (KN)
	P_v	P_v	P_v
3	-20	0	0
6	0	-20	0
9	0	0	-20



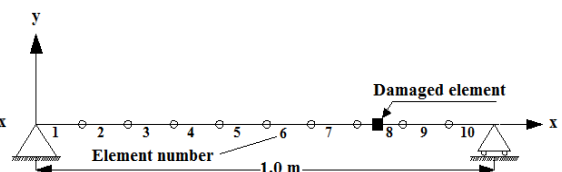
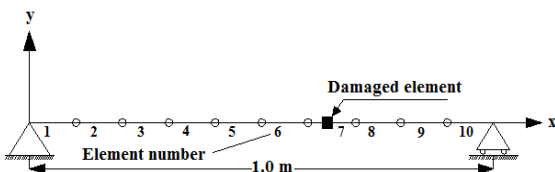
Case-1 Reduction in $h_3=20\%$

Case-2 Reduction in $h_4=25\%$



Case-3 Reduction in $h_5=15\%$

Case-4 Reduction in $h_6=10\%$



Case-5 Reduction in $h_7=30\%$

Case-6 Reduction in $h_8=10\%$

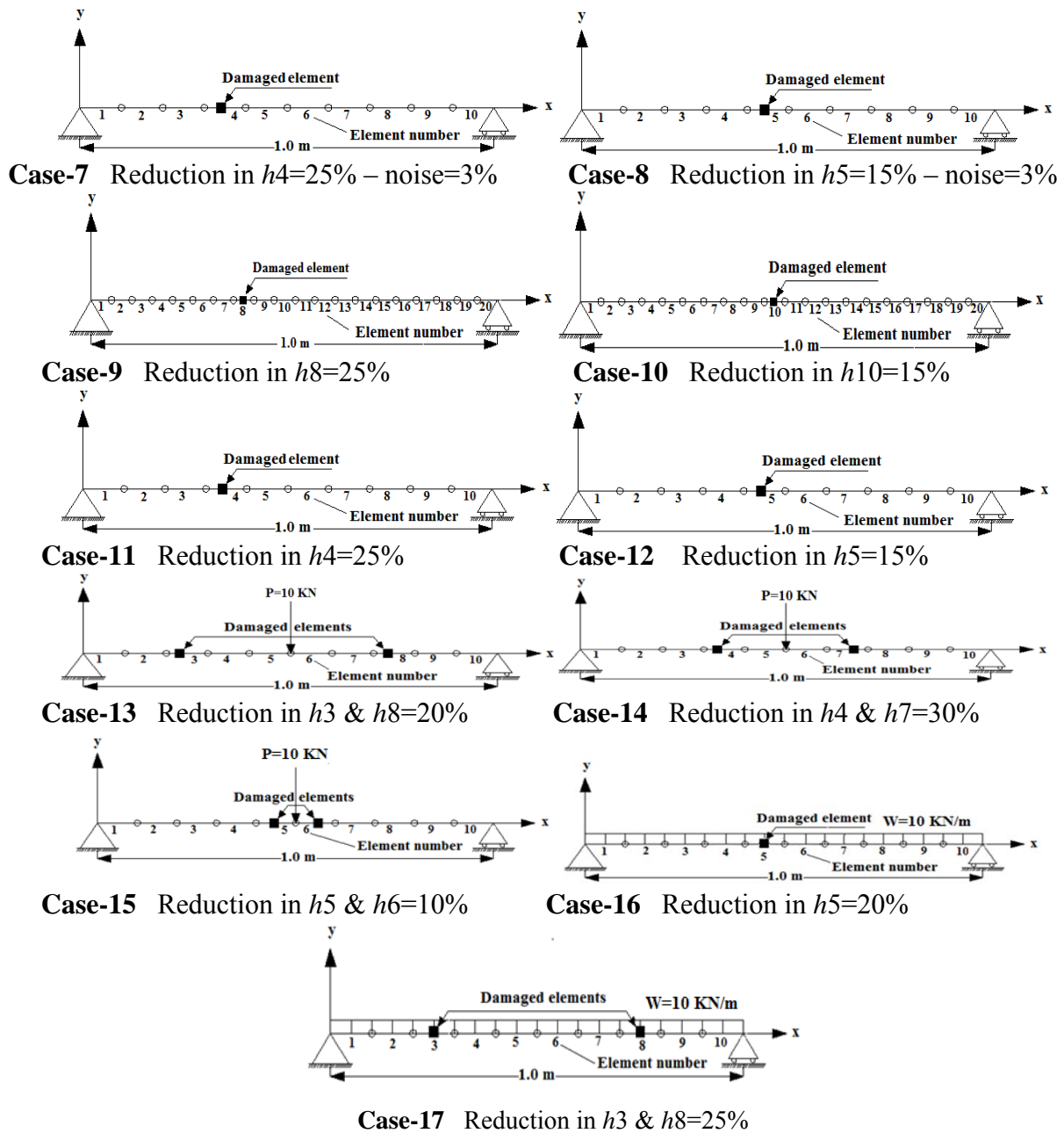


Figure 6. Seventeen different damage scenarios for the simply supported beam

For evaluating the index given by Eq. (18), the deflection equation of the beam before and after damage is needed to be determined. The curve fitting toolbox of MATLAB [25] is employed here for this purpose. For example, the deformed shape and corresponding equations obtained for the intact beam and damaged beam of case 14 are shown in Figures 7-8, respectively.

Damage identification charts of simply supported beam for cases 1-17 are shown in Figure 9. As shown in the figure, the value of $mnSRBI$ is further in vicinity of some elements that this indicates there is damage in these elements. The $mnSRBI$ is shown for damage scenarios 2 and 3 (with 10 elements) and 9 and 10 (with 20 elements) in Figures 9 (b)-(c) and 9 (i)-(j), respectively. The results show that the location of damage is identical in both cases. This means that the number of measurements is not very important, while the most important factor for determining the damage location is precise data and the accuracy of measurement.

However, for avoiding the false damage detection, it is suggested that the number of elements are not very low.

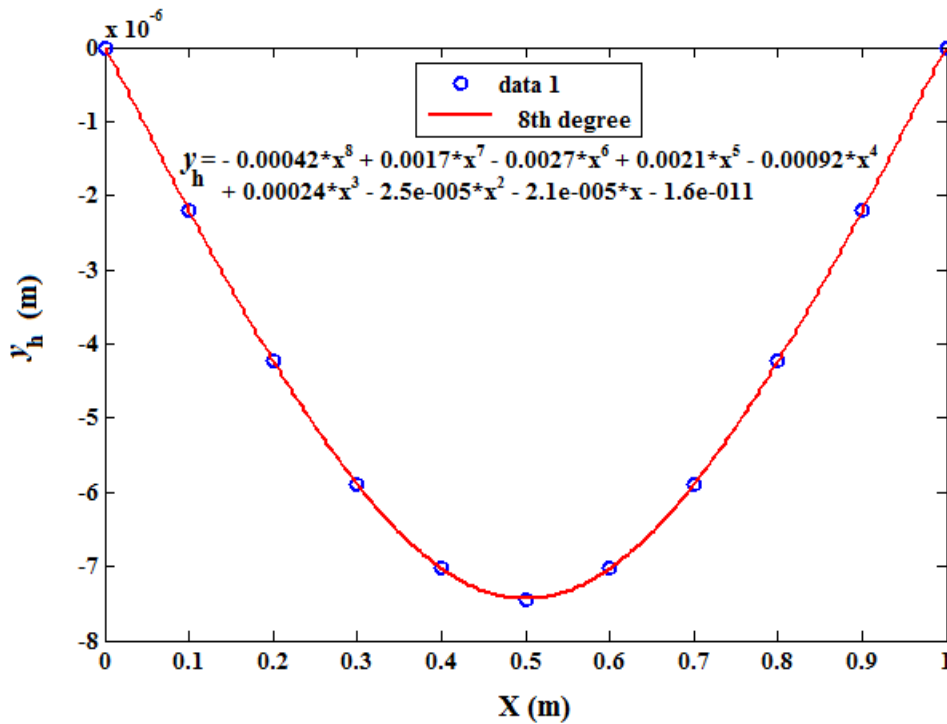


Figure 7. Deformed shape and deflection equation of the simply supported intact beam for case 14

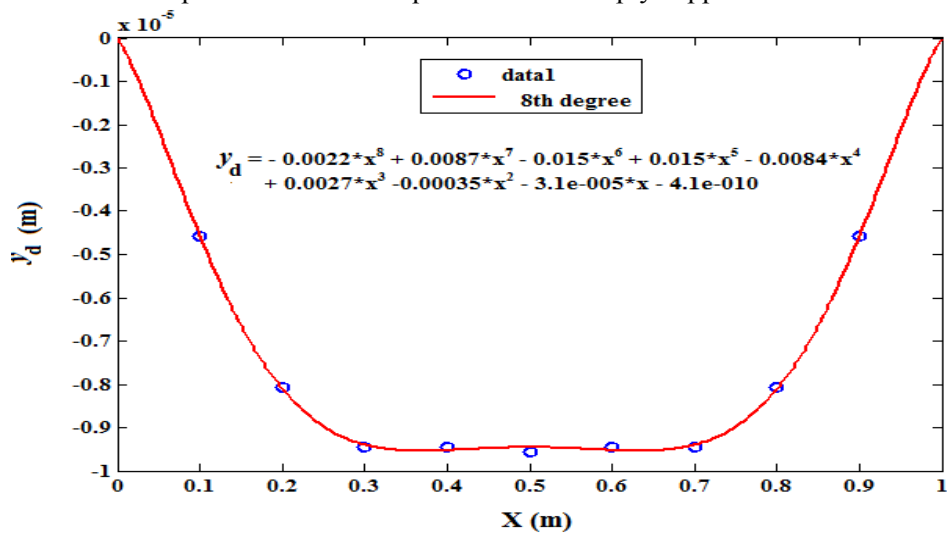
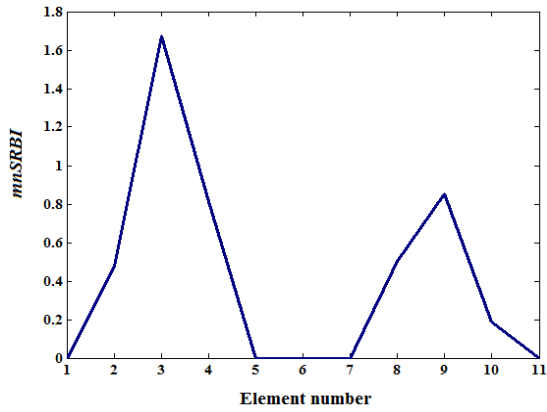
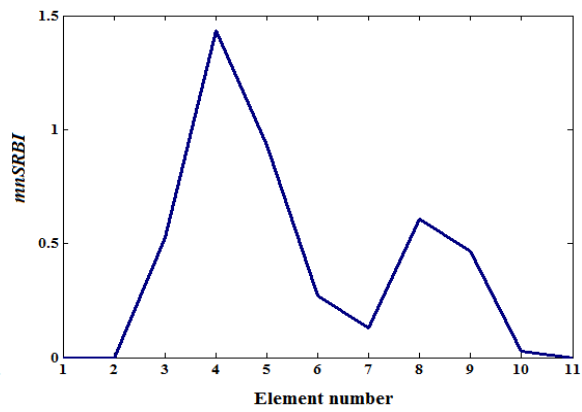


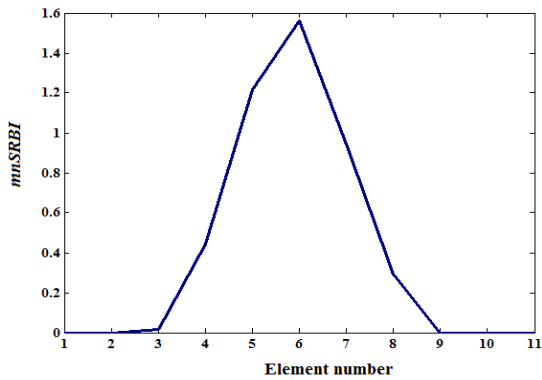
Figure 8. Deformed shape and deflection equation of the simply supported damaged beam for case 14



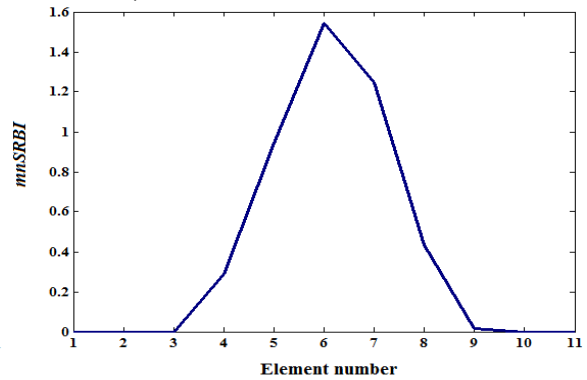
(a) Case-1 (damaged element=3, reduction in $h=20\%$)



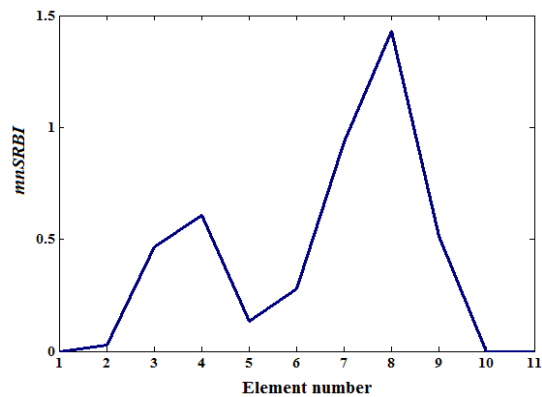
(b) Case-2 (damaged element=4, reduction in $h=25\%$)



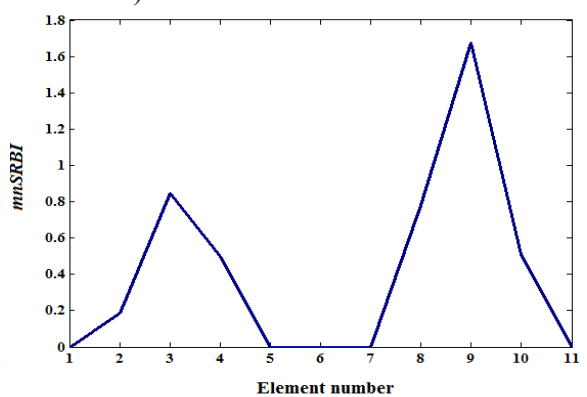
(c) Case-3 (damaged element=5, reduction in $h=15\%$)
reduction in $h=10\%$)



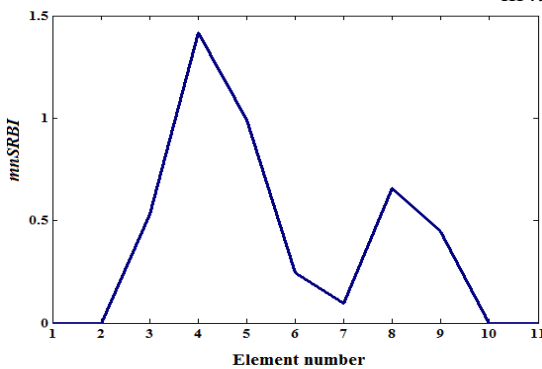
(d) Case-4 (damaged element=6, reduction in $h=10\%$)



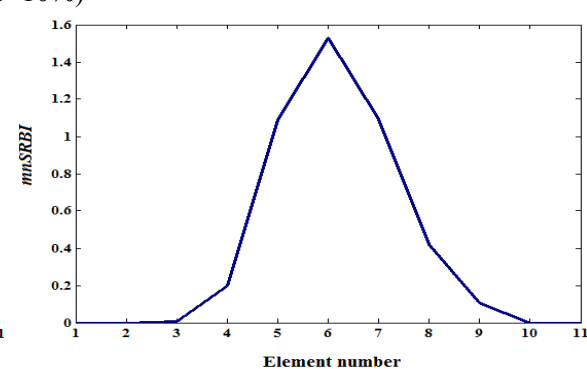
(e) Case-5 (damaged element=7, reduction in $h=30\%$)



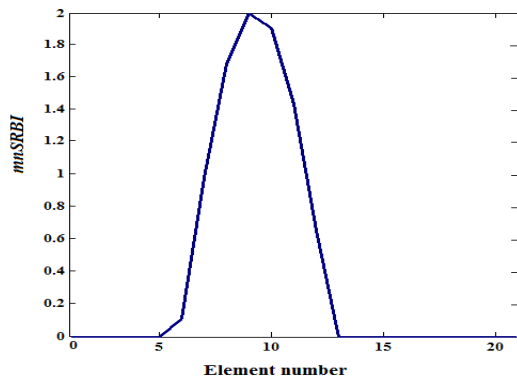
(f) Case-6 (damaged element=8, reduction in $h=10\%$)



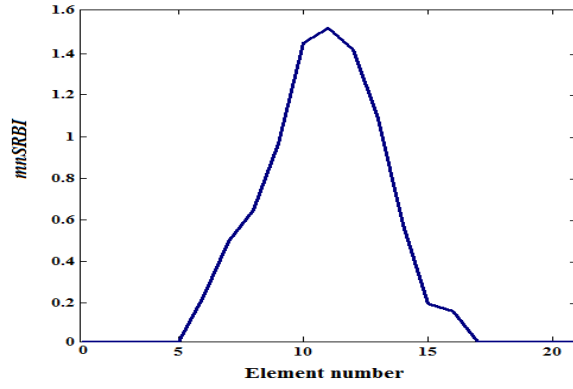
(g) Case-7 (damaged element=4, reduction in $h=25\%$, noise=3%)



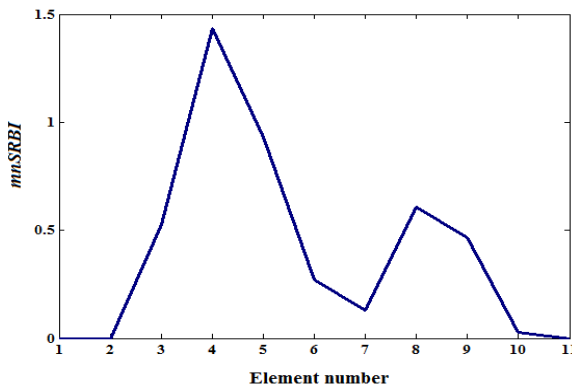
(h) Case-8 (damaged element=5, reduction in $h=15\%$, noise=3%)



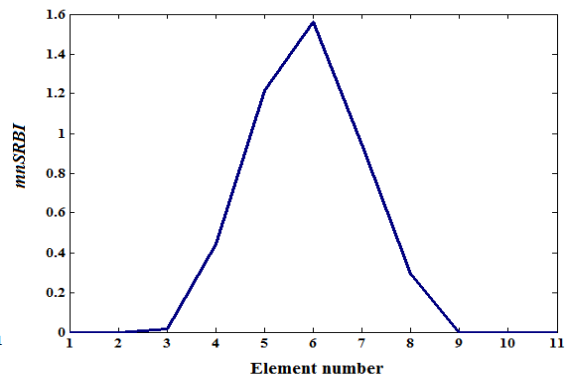
(i) **Case-9** (damaged element=8, reduction in $h=25\%$)



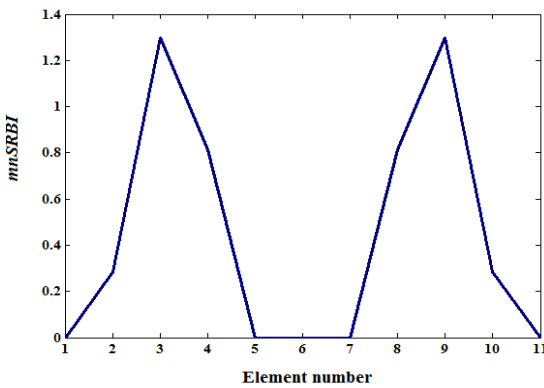
(j) **Case-10** (damaged element=10, reduction in $h=15\%$)



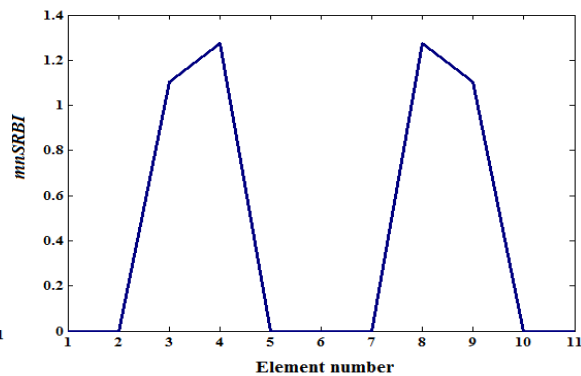
(k) **Case-11** (damaged element=4, reduction in $h=25\%$)



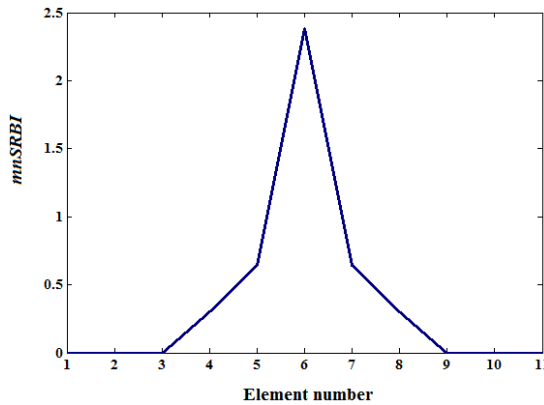
(l) **Case-12** (damaged element=5, reduction in $h=15\%$)



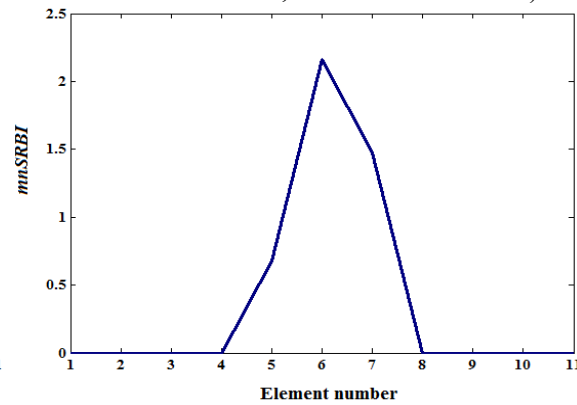
(m) **Case-13** (damaged elements=3 & 8, reduction in $h=20\%$)



(n) **Case-14** (damaged elements=4 & 7, reduction in $h=30\%$)



(o) **Case-15** (damaged elements=5 & 6, reduction in $h=10\%$)



(p) **Case-16** (damaged element=5, reduction in $h=20\%$)

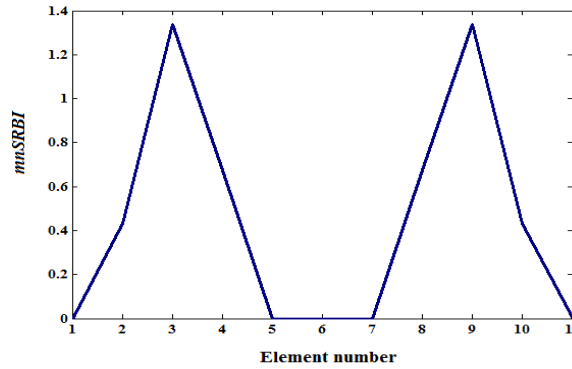
(q) Case-17 (damaged elements=3 & 8, reduction in $h=25\%$)

Figure 9. Damage identification of simply supported beam for cases 1-17

The values of $mnSRBI$ for damage scenarios 13-15 (multiple damages) are shown in Figures 9 (m)-(o), respectively. It is revealed that the index can also locate the multiple damage cases properly.

The values of $mnSRBI$ for damage scenarios 16-17 are shown in Figures 9 (p) and (q), respectively. The results show that the damage index can locate the single and multiple damages under uniformly distributed load correctly.

For examining the effect of load value on damage detection method, the results of scenario 2 and scenario 3 (use Table 1.) with scenario 11 and scenario 12 (use Table 3.), are compared, respectively. The identification charts are shown in Figures 9 (b)-(c) and 9 (k)-(l), respectively. As can be observed, the values of $SRBI$ are identical in both cases. In fact, the static responses for all measurements (nodes) in scenarios 11 and 12 are two times those obtained from scenario 2 and 3. This leads to double the values of numerator and denominator of $SRBI$. It can be concluded that the use of $SRBI$ as a method for determining the damage sites does not depend on load value. However, the magnitude of load plays an important role in practical work. In fact, the measurement devices may not be able to measure the static responses, when the applied loads are very small.

Figures 9 (g) and (h) show damage charts for the damage scenarios 7 and 8 considering 3% noise, respectively. When comparing them with those shown in Figures 9 (b) and (c) for scenarios 2 and 3 (states without noise), it can be indicated that there is a good compatibility between these values. In other words, the measured noise has a negligible effect on $SRBI$. It should be noted that for considering the stochastic nature of damage detection method with respect to randomly generated noise, a Mont Carlo simulation is required to be performed [15]. However, as the technique proposed here does not present a quantitative criterion to determine the correct damage detection needed for Mont Carlo simulations, so the mean of some different runs has been considered instead of a Mont Carlo simulation.

All of the results prove that the use of the static responses (nodal displacements, slope and displacement curvature) can be useful for identifying the damage of the beam. It seems that the method may be better than a vibration based method that needs more expensive sensors and in case of ambient vibration, will have a lot of noise [18].

5.2. Example 2: An overhanging beam

An overhanging beam with span $L=1$ m shown in Figure 10 is selected as second example. The beam has a square cross-section with dimensions of 0.2×0.2 m. Modulus of elasticity is $E = 210GPa$. As shown in Figure 11, eight different damage scenarios are considered for the beam. The first six scenarios (cases 1-6), include single damage case under concentrated load.

For damage scenarios 1-6, three different load cases as given in Tables 4-6 are considered. The Table 4, Table 5 and Table 6 are used to scenarios 1-4, scenario 5 and scenario 6, respectively.

The seventh and eighth scenarios (case 7 and 8) are considered for single and multiple damages under uniformly distributed load, respectively. In fourth scenario (case 4) noise effect is also considered. For studying the number of measurement point effect on the efficiency of damage detection method, two different finite element meshes are taken in scenarios 1-8. The first mesh consists of 10 elements (damage scenarios 1-8, except scenario 5, the length of each element is equal $0.1L$) and the second one includes 20 elements (damage scenario 5, the length of each element is equal $0.05 L$). The influence of amount of load is also considered. The scenario 6 is similar to scenario 1 excluding the value of the load has been two times. In this example, the 3% noise is considered in fourth scenario (case 4).

The values of $mnSRBI$ for damage scenarios 2 (with 10 elements) and 5 (with 20 elements) are shown in Figures 12 (b) and 12 (e), respectively. The results show that the location of damage is identical in both cases. This means that the number of measurement points cannot affect the results considerably, while the most important factor for determining the damage location is the accuracy of the measurement data. As shown in Figure 12, the $mnSRBI$ in the vicinity of some elements is maximal and it indicates that there is damage in the elements.

In order to examine the effect of the amount of load on damage detection method, the results of scenario 1 (use table 4) and scenario 6 (use table 6) are compared in Figures 12 (a) and (f), respectively. As can be observed, the $mnSRBI$ is the same for both the cases. It can be theoretically concluded that the use of $mnSRBI$ dose not depend on the value of load.

The values of $mnSRBI$ for damage scenarios 7-8 are shown in Figures 12 (g) and (h), respectively. The results show that the damage index can locate the single and multiple damages under uniformly distributed load correctly.

Figure 12 (d) show $mnSRBI$ for the damage scenario 4 considering 3% noise. By comparing this result with that shown in Figure 12 (a) for scenario 1, it can be concluded that there is a good compatibility between them. In other words, considering the measurement noise has a negligible effect on the performance of damage detection method.

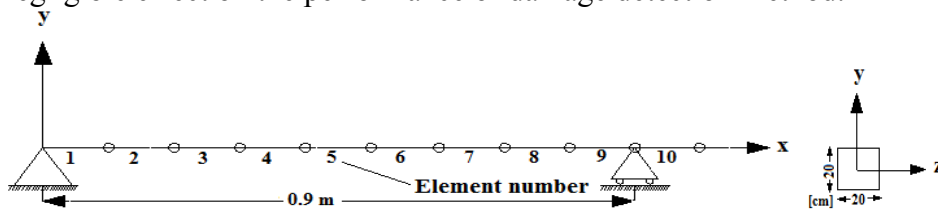


Figure 10. (a) Geometry of the overhanging beam (b) Cross-section of the beam

Table 4. Static load cases applied to the overhanging beam (scenarios 1-4)

Node	Case 1 (KN)		Case 2 (KN)		Case 3 (KN)	
	P_y		P_y		P_y	
3	-10		0		0	
6	0		-10		0	
9	0		0		-10	

Table 5. Static load cases applied to the overhanging beam (scenario 5)

Node	Case 1 (KN)	Case 2 (KN)	Case 3 (KN)
	P_v	P_v	P_v
5	-10	0	0
11	0	-10	0
17	0	0	-10

Table 6. Static load cases applied to the overhanging beam (scenario 6)

Node	Case 1 (KN)	Case 2 (KN)	Case 3 (KN)
	P_v	P_v	P_v
3	-20	0	0
6	0	-20	0
9	0	0	-20

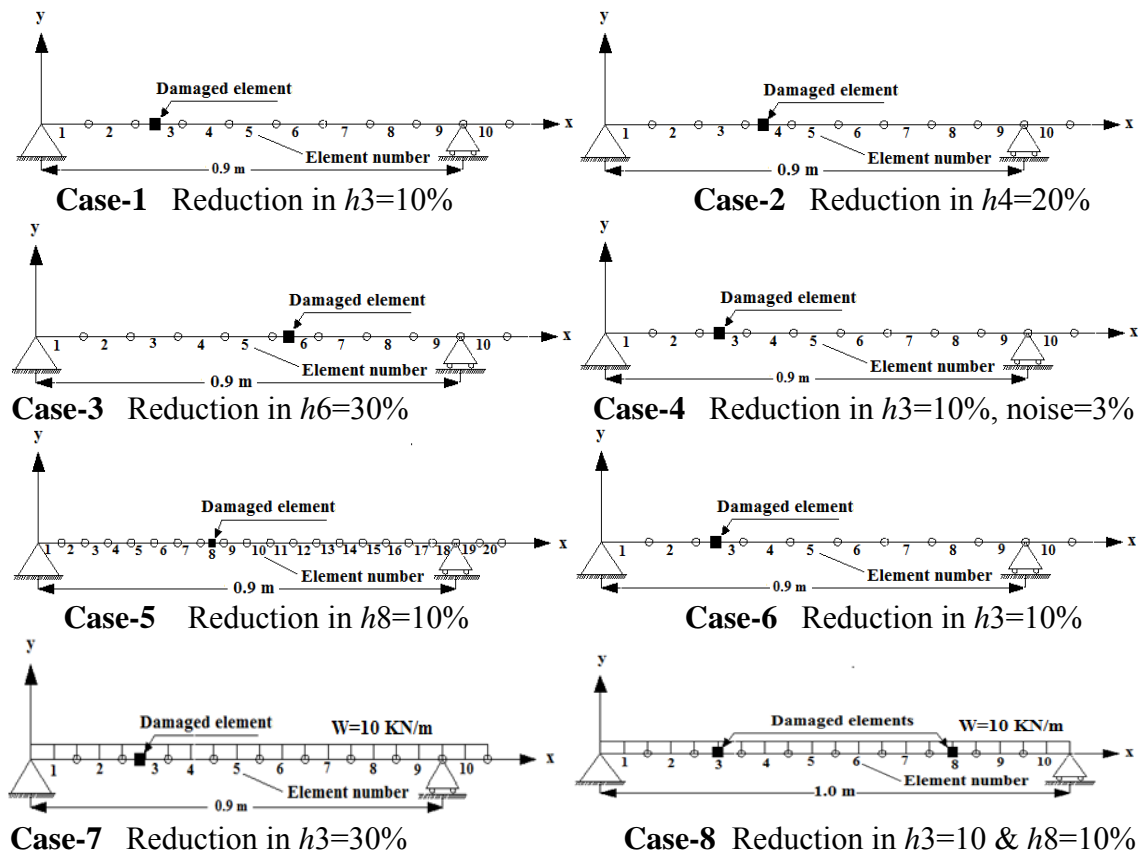
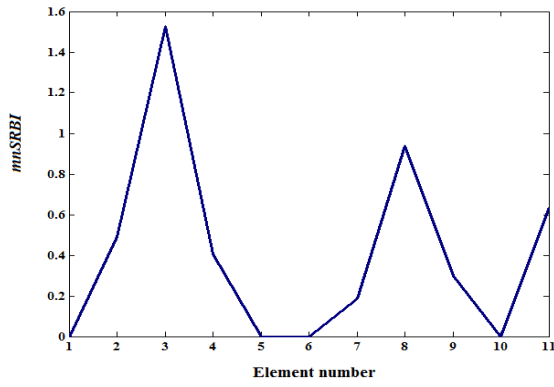
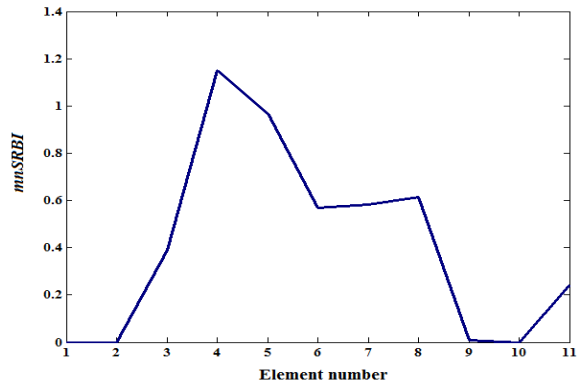


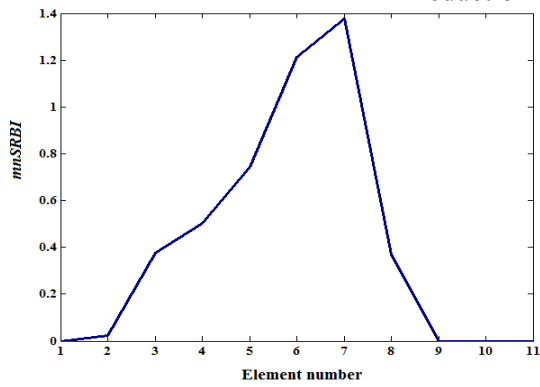
Figure 11. Eight different damage scenarios for the overhanging beam



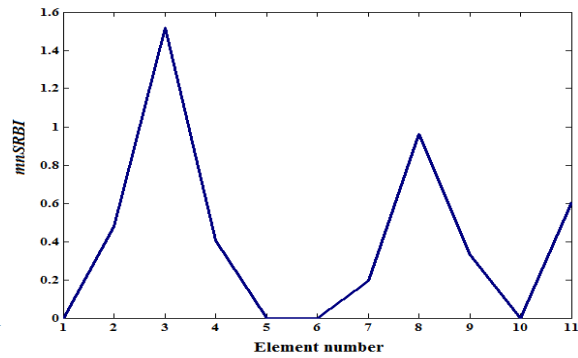
(a) Case-1 (damaged element=3, reduction in $h=10\%$)



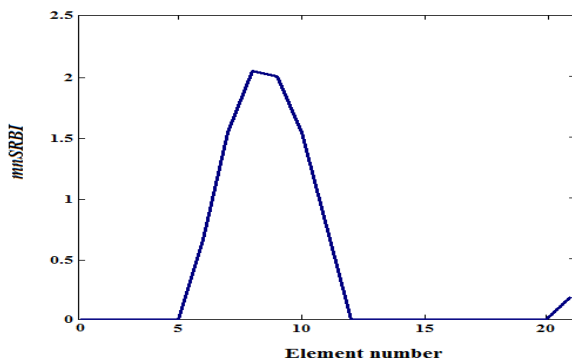
(b) Case-2 (damaged element=4, reduction in $h=20\%$)



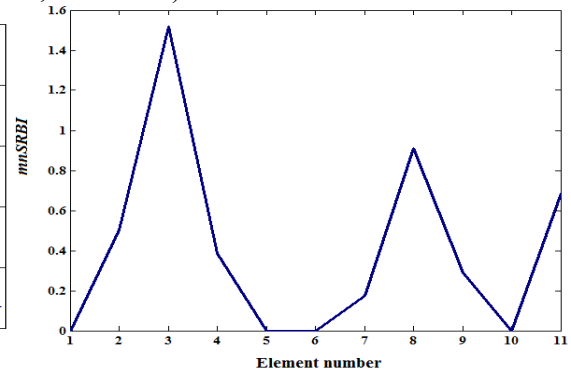
(c) Case-3 (damaged element=6, reduction in $h=30\%$)



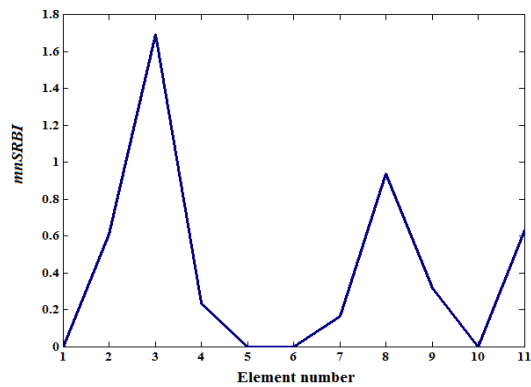
(d) Case-4 (damaged element=3, reduction in $h=10\%$, noise=3%)



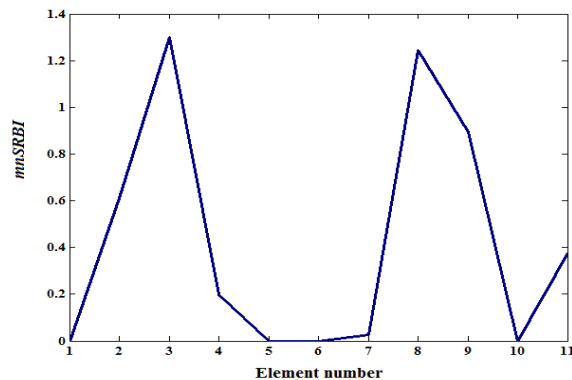
(e) Case-5 (damaged element=8, reduction in $h=10\%$)



(f) Case-6 (damaged element=3, reduction in $h=10\%$)



(g) Case-7 (damaged element=3, reduction in $h=30\%$)



(h) Case-8 (damaged elements=3&8, reduction in $h=10\%$)

Figure 12. Damage localization in overhanging beam for damage cases 1-8

5.3. Example 3: An indeterminate beam

An indeterminate beam with span $L=1$ m shown in Figure 13 is selected as the third example. The beam has a square cross-section with dimensions of 0.2×0.2 m. Modulus of elasticity is $E = 210GPa$. As shown in Figure 14, six different damage scenarios are considered for the beam. The first four scenarios (cases 1-4), include single damage case under concentrated load. For damage scenarios 1-4, three different load cases as given in Table 7 are considered.

The fifth and sixth scenarios (case 5 and 6) are considered for single and multiple damages under uniformly distributed load, respectively. In fourth scenario (case 4) noise effect is also considered. In this example, 3% noise is considered.

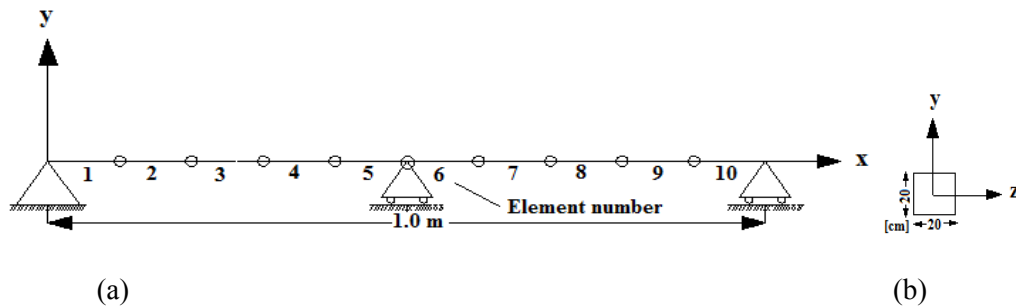


Figure 13. (a) Geometry of the indeterminate beam; (b) Cross-section of the beam

Table 7. Static load cases applied to the indeterminate beam (scenarios 1-4)

Node	Case 1 (KN)	Case 2 (KN)	Case 3 (KN)
	P_v	P_v	P_v
3	-10	0	0
5	0	-10	0
9	0	0	-10

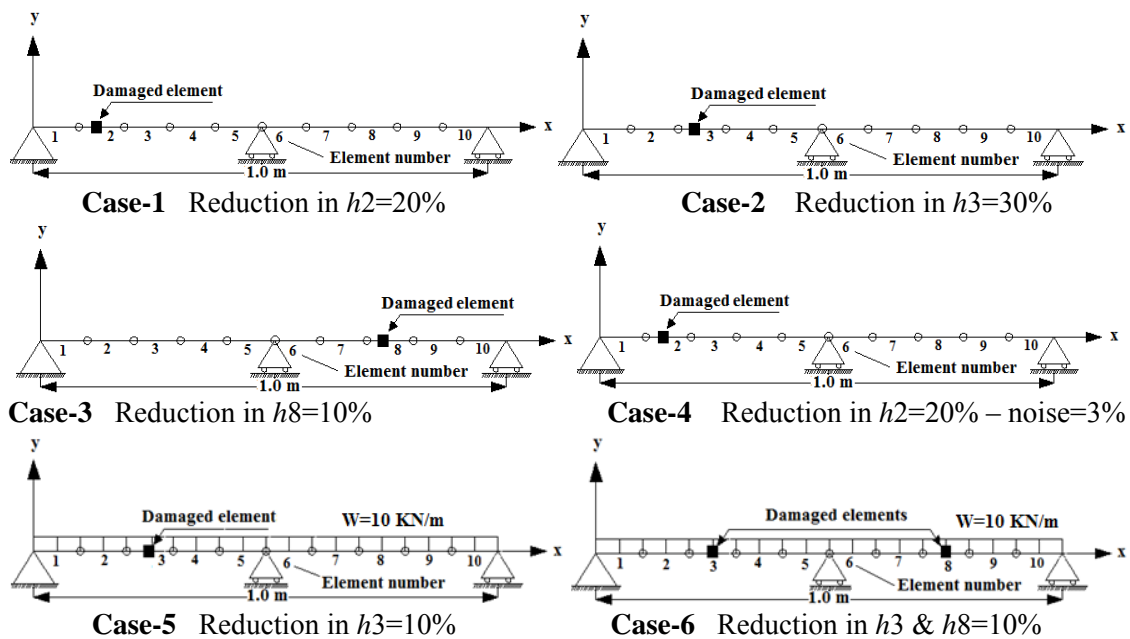
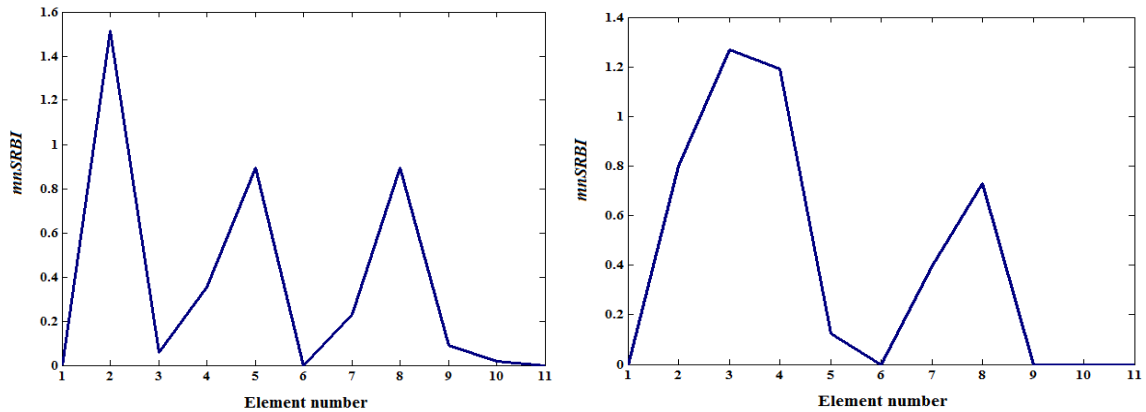


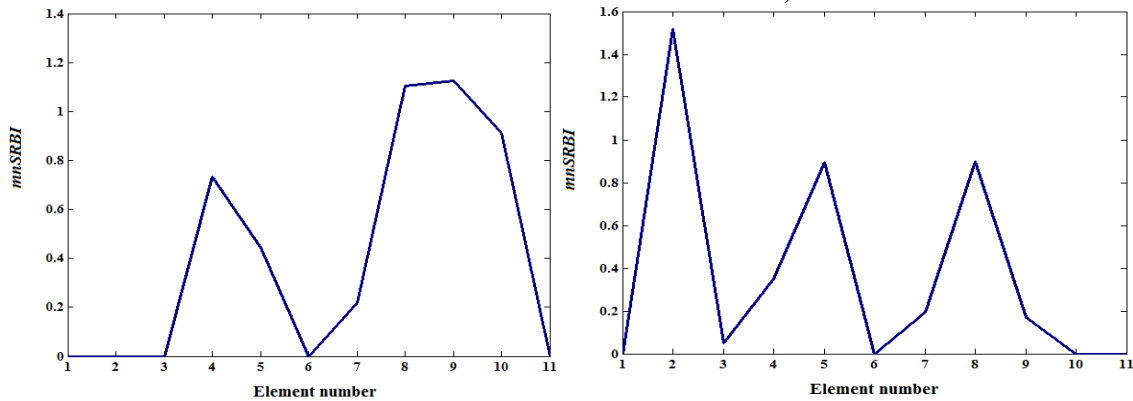
Figure 14. Six different damage scenarios for the indeterminate beam

As shown in Figure 15, the $mnSRBI$ in the vicinity of some elements is maximum and it indicates that there is damage in the elements.

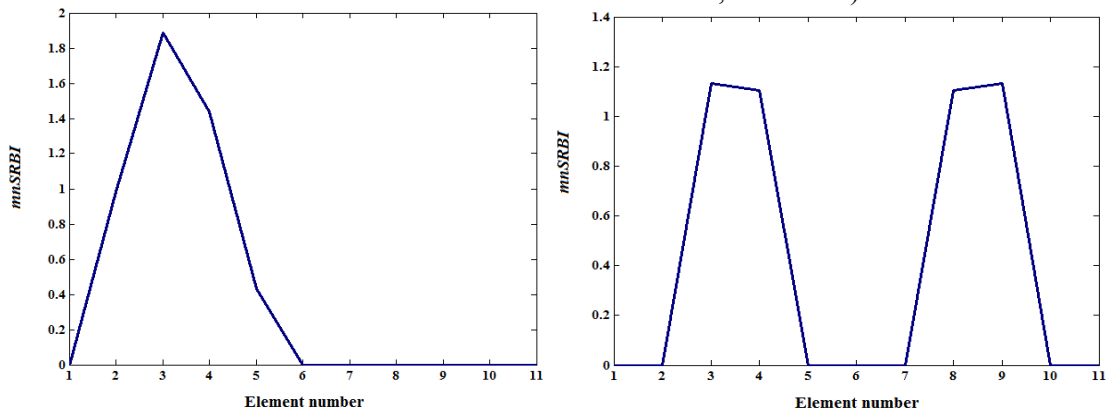
The values of $mnSRBI$ for damage scenarios 1-6 are shown in Figures 15 (a)-(f), respectively. The results confirm that the damage index can correctly determine the location of the single and multiple damages under concentrated and uniformly distributed load. Figure 15 (d) show $mnSRBI$ for the damage scenario 4 considering 3% noise. Comparing this result with that shown in Figure 15 (a) for scenario 1, it can be concluded that the method can accurately locate the damage when considering noise.



(a) Case-1 (damaged element=2, reduction in $h=20\%$) (b) Case-2 (damaged element=3, reduction in $h=30\%$)



(c) Case-3 (damaged element=8, reduction in $h=10\%$) (d) Case-4 (damaged element=2, reduction in $h=20\%$, noise=3%)



(e) Case-5 (damaged element=3, reduction in $h=10\%$) (f) Case-6 (damaged element=3 & 8, reduction in $h=10\%$)

Figure 15. Damage localization in indeterminate beam for damage cases 1-6

6. Conclusion

In this paper, a crack identification method for beams using an efficient damage index based on data extracted from a static analysis has been investigated. The effects of many parameters may affect the efficiency of the method with considering a simply supported beam, an overhanging beam and an indeterminate beam as test examples have been considered. Based on the numerical studies, the following results can be concluded:

- 1) Static responses obtained from the static analysis are sensitive to the stiffness reduction (moments of inertia). In other words, it has characteristics from damaged area and can be used as a good indicator for damage detection. It may fairly be better than a dynamical method that needs more expensive instruments.
- 2) As achieved from the numerical results, the number of measurement points is not very important, however, the most important factor is the accuracy of measurement. However, for increasing the accuracy of the proposed indicator, we suggest that the number of elements shouldn't be very low.
- 3) The proposed damage index does not depend on the location and amount of the static load and it can be effectively used for locating the single and multiple damage cases. However, the magnitude of load plays an important role in practical work. In fact, the measurement devices may not be able to measure the static responses, when the applied loads are very small.
- 4) Measurement noise has a negligible effect on the efficiency of the proposed index for damage detection.

References

- [1] R.D. Adams, P. Cawley, C.J. Pye, B.J. Stone, A Vibration technique for non- destructively assessing the integrity of structures, *Journal. Mechanical Engineering Science*, Vol. 20, 2 (1978), 93–100.
- [2] P.F. Rizos, N. Aspragathos, A. D. Dimarogonas, Identification of crack location and magnitude in a cantilever beam from the vibration modes, *Journal of Sound and Vibration*, Vol. 138, 3 (1990), 381–388.
- [3] A.K. Pandey, M. Biswas, Damage detection in structures using changes in flexibility, *Journal of Sound and Vibration*, Vol. 169, 1 (1994), 3–17.
- [4] D. Capecchi, F. Vestroni, Monitoring of structural systems by using frequency data, *Earthquake Engineering & Structural Dynamics*, Vol. 28, 5 (1999), 447–461.
- [5] F. Vestroni, D. Capecchi, Damage detection in beam structures based on frequency measurements, *Journal of Engineering Mechanics*, Vol. 126, 7 (2000), 761–768.
- [6] H.P. Chen, N. Bicanic, Assessment of damage in continuum structures based on incomplete modal information, *Computers & Structures*, Vol. 74, 5 (2000), 559–570.
- [7] P.F. Pai, L.G. Young, Damage detection of beams using operational deflection shapes, *International Journal of Solids and Structures*, Vol. 38, 18 (2001), 3161–3192.
- [8] M.A.-B Abdo, M. Hori, A numerical study of structural damage detection using changes in the rotation of mode shapes, *Journal of Sound and Vibration*, Vol. 251, 2 (2002), 227–239.
- [9] H.W. Shih, D.P. Thambiratnam and T.H.T. Chan, Vibration based structural damage detection in flexural members using multi-criteria approach, *Journal of Sound and Vibration*, Vol. 323, 3-5 (2009), 645–661.
- [10] S.M. Seyedpoor, Structural damage detection using a multi-stage particle swarm optimization, *Advances in Structural Engineering*, Vol. 14, 3 (2011), 533-549.
- [11] S. Moradi, P. Razi, L. Fatahi, On the application of bees algorithm to the problem of crack detection of beam-type structures, *Computers and Structures*, Vol. 89, 23-24 (2011), 2169–2175.
- [12] S.M. Seyedpoor, A two stage method for structural damage detection using a modal strain energy based index and particle swarm optimization, *International Journal of Nonlinear Mechanics*, Vol. 47, 1 (2012), 1-8.
- [13] M. Nobahari, S.M. Seyedpoor, An efficient method for structural damage localization based on the concepts of flexibility matrix and strain energy of a structure, *Structural Engineering and Mechanics*, Vol. 46, 2 (2013), 231-244.

- [14] M.R. Banan, M.R. Banan, K.D. Hjelmstad, Parameter estimation of structures from Static Response, II: Numerical simulation, *Journal of Structural Engineering*, Vol. 120 11 (1994), 3259-3283.
- [15] M. Sanayei, M.J. Saletnik, Parameter estimation of structures from static strain measurements II: Error sensitivity analysis, *Journal of Structural Engineering, ASCE*, Vol. 122, 5 (1996), 563-572.
- [16] X. Wang, N. Hu, Hisao Fukunaga and Z.H. Yao, Structural damage identification using static test data and changes in frequencies, *Engineering Structures*, Vol. 23, 6 (2001), 610–621.
- [17] F. Bakhtiari-Nejad, A. Rahai, A. Esfandiari, A structural damage detection method using static noisy data, *Engineering Structures*, Vol. 27, 12 (2005), 1784-1793.

- [18] X.Z. Chen, H.P. Zhu, C.Y. Chen, Structural damage identification using test static data based on grey system theory, *Journal of Zhejiang University SCIENCE*, Vol. 6A, 8 (2005), 790–796.
- [19] S. Caddemi and A. Morassi, Crack detection in elastic beams by static measurements, *International Journal of Solids and Structures*, Vol. 44, 16 (2007), 5301–5315.
- [20] M. A.-B. Abdo, Parametric study of using only static response in structural damage detection, *Engineering Structures*, Vol. 34, (2012), 124-131.
- [21] Seyedpoor S.M., O. Yazdanpanah, An efficient indicator for structural damage localization using the change of strain energy based on static noisy data, *Applied Mathematical Modeling*, Vol.38, 9–10 (2014), 2661–2672.
- [22] F.P. Beer, E.R. Johnston, Jr., J.T. DeWolf, *Mechanics of Materials*, 3rd Edition, McGraw-Hill, New York, 2002.
- [23] S.S. Samaee, O. Yazdanpanah and D.D. Ganji, Homotopy perturbation method and parameterized perturbation method for radius of curvature beam equation, *International Journal of Computational Materials Science and Engineering*, Vol. 1, 4 (2012), DOI: 10.1142/S2047684112500339.
- [24] J.K. Sinha, M.I. Friswell, S. Edwards, Simplified models for the location of cracks in beam structures using measured vibration data, *Journal of Sound and Vibration*, Vol. 251, 1 (2002), 13–38.
- [25] MATLAB, *The language of technical computing (software)*, Math Works Inc., (R2010b).